Quantum computation in brain microtubules: Decoherence and biological feasibility

S. Hagan,[1] S. R. Hameroff,[2] and J. A. Tuszyński[3]
[1]*Department of Mathematics, British Columbia Institute of Technology, Burnaby, British Columbia, Canada V5G 3H2*
[2]*Departments of Anesthesiology and Psychology and Center for Consciousness Studies, University of Arizona, Tucson, Arizona 85724*
[3]*Department of Physics, University of Alberta, Edmonton, Alberta, Canada T6G 2J1*
(Received 2 May 2000; revised manuscript received 7 August 2001; published 10 June 2002)

The Penrose-Hameroff orchestrated objective reduction (orch. OR) model assigns a cognitive role to quantum computations in microtubules within the neurons of the brain. Despite an apparently ''warm, wet, and noisy'' intracellular milieu, the proposal suggests that microtubules avoid environmental decoherence long enough to reach threshold for ''self-collapse'' (objective reduction) by a quantum gravity mechanism put forth by Penrose. The model has been criticized as regards the issue of environmental decoherence, and a recent report by Tegmark finds that microtubules can maintain quantum coherence for only 10^{-13} s, far too short to be neurophysiologically relevant. Here, we critically examine the decoherence mechanisms likely to dominate in a biological setting and find that (1) Tegmark's commentary is not aimed at an existing model in the literature but rather at a hybrid that replaces the superposed protein conformations of the orch. OR theory with a soliton in superposition along the microtubule; (2) recalculation after correcting for differences between the model on which Tegmark bases his calculations and the orch. OR model (superposition separation, charge vs dipole, dielectric constant) lengthens the decoherence time to 10^{-5}–10^{-4} s; (3) decoherence times on this order invalidate the assumptions of the derivation and determine the approximation regime considered by Tegmark to be inappropriate to the orch. OR superposition; (4) Tegmark's formulation yields decoherence times that increase with temperature contrary to well-established physical intuitions and the observed behavior of quantum coherent states; (5) incoherent metabolic energy supplied to the collective dynamics ordering water in the vicinity of microtubules at a rate exceeding that of decoherence can counter decoherence effects (in the same way that lasers avoid decoherence at room temperature); (6) microtubules are surrounded by a Debye layer of counterions, which can screen thermal fluctuations, and by an actin gel that might enhance the ordering of water in bundles of microtubules, further increasing the decoherence-free zone by an order of magnitude and, if the dependence on the distance between environmental ion and superposed state is accurately reflected in Tegmark's calculation, extending decoherence times by three orders of magnitude; (7) topological quantum computation in microtubules may be error correcting, resistant to decoherence; and (8) the decohering effect of radiative scatterers on microtubule quantum states is negligible. These considerations bring microtubule decoherence into a regime in which quantum gravity could interact with neurophysiology.

DOI: 10.1103/PhysRevE.65.061901 PACS number(s): 87.16.Ka, 87.15.−v, 03.67.Lx, 04.60.−m

I. INTRODUCTION

In the conventional biophysical approach to understanding cognitive processes, it has been generally accepted that the brain can be modeled, according to the principles of classical physics, as a neural network [1–5]. Investigations in this field have delivered successful implementations of learning and memory along lines inspired by neural architectures and these have promoted optimism that a sufficiently complex artificial neural network would, at least in principle, incur no deficit in reproducing the full spectrum and extent of the relevant brain processes involved in human cognition and consciousness.

However, physical effects in the functioning of the nervous system, which lie outside the realm of classical physics, suggest that such simulations may ultimately prove insufficient to the task. One finds ample support for this in an analysis of the sensory organs, the operation of which is quantized at levels varying from the reception of individual photons by the retina [6,7] to thousands of phonon quanta in the auditory system [8]. Of further interest is the argument that synaptic signal transmission has a quantum character [9,10], although the debate on this issue has not been conclusive [11]. We note that using the thermal energy at room temperature in the position-momentum uncertainty relation, and assuming a 1 Å uncertainty for quantal effects, Beck and Eccles [9] concluded that a particle whose mass is just six proton masses would cease to behave quantum mechanically and become classical for all intents and purposes. This seems a serious underestimate, based on the de Broglie wavelength alone. In any case, it is known that quantum modes of behavior exist in much larger structures, such as peptides, DNA, and proteins [12]. For instance, Roitberg *et al.* [13] demonstrated functional protein vibrations that depend on quantum effects centered in two hydrophobic phenylalanine residues, and Tejada *et al.* [14] have evidence to suggest that quantum coherent states exist in the protein ferritin. Finally, new developments in magnetic resonance imaging of the brain demonstrate that induced quantum coherences of proton spins separated by distances ranging from micrometers to 1 mm are sustained for tens of milliseconds and longer [15–17]. While these unentangled quantum couplings are not the type of quantum processes that are likely to prove useful in brain function, they nonetheless demonstrate that mesoscopic quantum coherence can indeed survive in the brain's milieu. Similarly, the aforementioned quantum

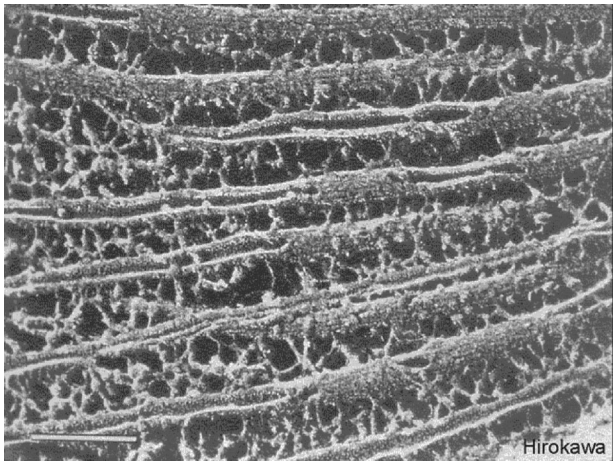

FIG. 1. Immunoelectron micrograph of dendritic microtubules interconnected by microtubule-associated proteins (MAPs). Some microtubules have been sheared, revealing their hollow inner core. Scale bar at lower left represents 100 nm. With permission from Hirokawa [79].

modes in peptides, DNA, and proteins are not the stable, entangled superpositions required for quantum computation, but show that biology can take advantage of quantum modes in clever ways.

The inadequacy of classical treatments is further suggested at the cognitive level, not only as regards longstanding difficulties related to, for instance, accounts of semantics [18], binding [19], and the neural correlate of consciousness, but even in the rather modest goal of reproducing cognitive computational characteristics. Penrose, in particular, has argued that human understanding must involve a noncomputational element [20,21] inaccessible to simulation on classical neural networks and this might be realized through a biological instantiation of quantum computation.[1] Along these lines, Penrose and Hameroff have put forth a specific model [22–24]—orchestrated objective reduction (orch. OR)—positing quantum computation in microtubule protein assemblies in the neurons of the brain.

Microtubules are hollow cylinders whose walls consist of 13 columns (protofilaments) of the protein tubulin arranged in a skewed hexagonal lattice (see Fig. 1). Along with other structures, microtubules comprise the internal scaffolding—the ''cytoskeleton''—in cells including neurons. Determinants of both structure and function, cytoskeletal structures are dynamically active, performing a host of activities instrumental to cellular organization and intelligence [25]. Earlier models (see, for instance, [26–32]) proposed classical information processing among the tubulin ''dimers'' composing microtubules—molecular-level automata regulating real-time cellular behavior. More recently, arguments have been made for quantum computation at the level of individual proteins [33]. In particular, functional protein conformational states are mediated by quantum van der Waals (London) forces [34], the relevance of which is demonstrated by the mechanism of action of the general anesthetic gases that reversibly ablate consciousness. Anesthetics act by disturbing such forces in the hydrophobic pockets of various brain proteins [35,36]. Microtubules are thus poised to mediate between a tubulin-based quantum computation and the classical functioning of neurons.

The Penrose-Hameroff proposal suggests that coherent superpositions of tubulin proteins are inherently unstable and subject to self-collapse under a quantum gravitational criterion (Penrose objective reduction or OR). In the orch. OR model [22,23], the phase of quantum superposition/computation is a preconscious process, and each self-collapse event corresponds to an instantaneous ''moment of conscious experience.'' The mode of collapse, i.e., the fate of proposed superpositions, is a separate issue, the question here being the duration of microtubule quantum states in the face of environmental decoherence. To have an impact on cognitive processes, microtubule superpositions need to survive long enough to interact with the brain's neurophysiological events, typically in the range of milliseconds to hundreds of milliseconds. Calculations indicate that superpositions of these durations would indeed reach self-collapse by quantum gravity in the context of the brain [22,23,37,38]. Quantum coherence that persists, or has influence over such a neurophysiologically relevant time frame, could regulate neural processes, in a manner accounting for the noncomputational element, by ''orchestrating'' state vector reductions to perform quantum computation.

According to the orch. OR model, the neuronal cytoplasm in which microtubules are embedded alternates between phases of (1) isolated quantum superposition/computation (solid, or gelatinous ''gel,'' actin polymerization) and (2) classical states of input/output communication (liquid solution or ''sol''). The input to and output from each OR event evolve as classical microtubule cellular automata—in the form of patterns of tubulin conformational states—to regulate synaptic function, membrane activities, and attachment sites for microtubule-associated proteins (MAPs). Input from synaptic activities may be provided by metabotropic receptors, which interface between membrane synaptic functions and the internal cytoskeleton/microtubules. For example, when the prevalent brain neurotransmitter acetylcholine binds to its postsynaptic receptor, a cascade of activities results in the microtubule-associated protein MAP2 decoupling from microtubules. Woolf [39] has suggested that such decoupling initiates isolation of quantum states in microtubules from the membrane and outside environment. MAPs also interconnect microtubules in bundles, or networks, and are suggested to regulate, or orchestrate, microtubule quantum states prior to OR by their particular attachment sites on the microtubular lattice.

An apparent vulnerability of the orch. OR model and other models of quantum processes relevant to cognition is the question of environmental decoherence. Specifically, can environmental decoherence be avoided and quantum super-

[1]It has been noted that fundamentally analog mechanisms, based on continuous rather than traditional discrete (Turing) computation, might also constitute noncomputation in the relevant sense and equally evade Penrose's argument. However, the essentially discrete nature of exocytosis implies that no such description can be framed in terms of the neurochemical basis of synaptic function.

position sustained long enough for the system to reach threshold for OR? In the original orch. OR formulation, it was assumed that decoherence would have to be avoided for periods long enough to be consistent with membrane electrophysiological events, i.e., 10^{-3}–10^{0} s. However, it has been suggested recently [40] that orch. OR events of far briefer duration may be sufficient. For example, sequences of many orch. OR events in the range of 10^{-7}–10^{-6} s may culminate in electrophysiological events in the 10^{-2}–10^{0} s range.

Recently, Tegmark [41] has responded to this and other models of brain function invoking a quantum element by contending that the relevant degrees of freedom cannot reasonably be sufficiently shielded from environmental, and particularly thermal, influence to maintain quantum superpositions until self-collapse. It is well known that technological quantum devices often require extremely low temperatures to avoid decoherence through environmental interaction. The survival of a delicate quantum coherence in the warm, wet, and noisy milieu of the brain long enough for quantum computation to play a neurophysiological role, therefore, seems unlikely to many observers. Tegmark maintains that orthodox mechanisms of decoherence would destroy a superposed microtubule-associated quantum state on a time scale of the order of 10^{-13} s, much shorter than that associated with events, such as neural firings. In the following, we critically review the assumptions, calculations, and claims that have been made in order to ascertain whether existing treatments accurately reflect the potential for quantum computation in the brain.

II. DECOHERENCE RATES

Tegmark considers in his paper [41] two different scales at which quantum computation might occur in the brain—one involving superpositions of neurons firing and not firing (with calculated decoherence times of 10^{-20} s), and another involving microtubules (calculated decoherence times of 10^{-13} s). We agree that superpositions at the level of neural firing are unlikely, and in fact play no role in the orch. OR or any other contemporary quantum model. In the orch. OR approach, neural firings are entirely classical, though they may be initiated by the outputs of microtubule quantum processes in the neuronal interior. We therefore focus our attention on Tegmark's assertions regarding decoherence times for microtubule-associated quantum superpositions.

Though Tegmark specifically implicates Penrose, his criticisms target neither the Penrose-Hameroff orch. OR model—the only detailed, quantitative model of quantum processes in microtubules with which Penrose is associated—nor any other that is currently or has been under investigation. His remarks appear to be directed against a spuriously quantum version of a classical model, put forth by Sataric *et al.* [29], to treat lossless energy transfer in microtubules in terms of kink solitons traveling along their length.

Tegmark considers a model in which kink soliton solutions, such as those of Sataric *et al.* [29], exist in a quantum superposition of different positions along the microtubule. The actual orch. OR model, on the other hand, is framed in terms of superpositions of the conformational state of a tubulin dimer, as illustrated in Fig. 2, in which superposition separation occurs at the level of each of the protein's atomic nuclei. The separated states are coupled to delocalizable electrons residing in the hydrophobic pocket of the tubulin dimer protein, pointing to a process of conformational change in the dimer controlled by quantum van der Waals (London) forces. There is thus a considerable conceptual disparity between this model and that considered by Tegmark. Nevertheless, it is equally critical to the actual orch. OR model that the mechanisms of decoherence analyzed do not destroy quantum coherence prematurely, before a quantum gravity-induced self-collapse can come into play. Below, we consider both numerical and theoretical concerns that bear on the results presented by Tegmark.

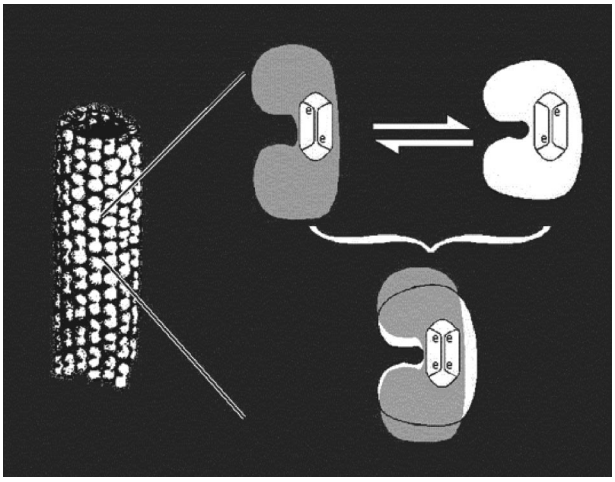

FIG. 2. Each tubulin dimer composing a microtubule can switch between two (or more) conformations coupled to van der Waals (London) forces in the hydrophobic pocket of each. In the orch. OR model, it is posited that tubulin can also exist in a superposition of both conformational states.

In the microtubule case, Tegmark determines the time to decoherence, τ, due to the long-range electromagnetic influence of an environmental ion to be

$$\tau \sim \frac{4\pi\epsilon_0 a^3\sqrt{mkT}}{Nq_e^2 s}, \tag{1}$$

where T is the temperature, m is the mass of the ionic species, a is the distance to the ion from the position of the superposed state, N is the number of elementary charges comprising that state, and s is the maximal ''separation'' between the positions of the tubulin mass in the alternative geometries of the quantum superposition. Since any difference in the mass distributions of superposed matter states will impact upon the underlying space-time geometry, such alternative geometries must presumably be permitted to occur within the superposition.

A. Superposition separation

Superposition occurs not only at the level of a mass distribution separated from itself, but concomitantly at the level of the underlying space-time geometry. According to Pen-

rose's quantum gravitational criterion for objective reduction, superpositions involving different space-time geometries are considered inherently unstable, with the rate of collapse determined by a measure of difference in the geometries. As this measure approaches the order of a Planck length, it becomes problematic to determine a consistent standard by which to match up points in the superposed geometries. Yet if the superposed spaces cannot be resolved into one and the same space, then the different matter states in the superposition must occur in separate spaces and the meaning of superposition in this context becomes obscure. Thus the rate of collapse in Penrose's suggestion for objective reduction must become significant before the measure of difference in superposed space-time geometries grows to the Planck scale. Since gravitational forces are inherently weak, however, the mass distributions of the superposed matter states can be substantially ''separated'' before incurring a large measure of difference in the associated space-time geometries.

Tegmark assumes that this separation s must be at least as large as the diameter of a microtubule, $D=24$ nm, for superpositions spanning many tubulin dimers. This estimate is based on a picture of tubulin dimers literally ''beside themselves'' in superposition. However, in the orch. OR theory, the authors contemplate separation only at the level of the individual atomic nuclei of amino acids comprising the protein.

Hameroff and Penrose [42] surveyed three different levels at which separation related to the protein conformational state of the tubulin dimers might occur: (1) partial separation (10%) of protein spheres, (2) complete separation of atomic nuclei, and (3) complete separation of nucleons. The gravitational self-energy in each instance is taken to be inversely proportional to the decoherence time according to the energy-time uncertainty relation. In the case of protein spheres, the energy E for partial separation is obtained from

$$E=\frac{GM^2s^2}{2r^3}\left(1-\frac{3s}{8r}+\frac{s^3}{80r^3}\right), \tag{2}$$

where M is the monomer mass of 55 kDa, r is the radius of a monomer sphere, and $s=\frac{1}{10}r$ is the superposition separation. For complete separations at the level of either atomic nuclei or nucleons, the contribution to the self-energy determined in separating the mass distributions to a distance of one diameter (the contact position in a spherical approximation of the masses) is of the same order as that determined by increasing the separation further, even to infinity, so the contribution in moving from coincidence to contact is a good order of magnitude estimator of the self-energy for complete separations.

Mass separation of granular arrays of atomic nuclei yields the highest energies of the three cases, and hence the shortest decoherence times, and it is this level that will thus dominate in an orchestrated reduction.[2] Thus mass separation is effected at separations the size of the nucleus, on the order of femtometers, some seven orders of magnitude smaller than Tegmark's estimate.

B. Polarization and charge

In his analysis of the polarization associated with the microtubule, Tegmark defines $p(x)$ to be the average component, in the direction parallel to the microtubule axis, of the electric dipole moment due to the tubulin dimers, a polarization function given in units of (charge) $\times$ (length). The subsequent claim that $-p'(x)$ represents the net charge per unit length along the microtubule, cannot then, on dimensional grounds alone, be well founded. Nevertheless, on this basis, Tegmark integrates over the length of the microtubule across the kink to obtain a net charge that incorrectly bears the units of an electric dipole moment. This, in effect, treats the microtubule as a line of uniform charge rather than a polarized line, and this is how he obtains the magnitude of the *polarization* function by simply summing the *charge* of the ions arrayed around the microtubule at the level of the kinklike propagation. The value of N that figures in his estimate of the decoherence time is then this sum expressed in units of the electron charge q_e. Aside from the dimensional incongruities in this procedure, Tegmark accounts only for the presence of 18 Ca^{2+} ions, bound to the C terminus of the tubulin on each of 13 protofilaments in a cross section of the microtubule. This overlooks the negative charges borne by amino acid side groups and numerous other charges associated with tubulin, all of which attract counterions from the surrounding medium.

Tubulin has been imaged to atomic resolution only within the last two years, following 20 years of difficult work with this protein. Nogales *et al.* published the structure of α- and β-tubulin, co-crystallized in the heterodimeric form [44]. The work establishes that the structures of α and β tubulin are nearly identical and confirms the consensus speculation. A detailed examination shows that each monomer is formed by a core of two β sheets that are surrounded by α helices. The monomer structure is very compact, but can be divided into three functional domains: the amino-terminal domain containing the nucleotide-binding region, an intermediate domain containing the taxol-binding site, and the carboxy-

[2]Estimates of the time to self-collapse (decoherence time) due to such a quantum gravitational mechanism will depend on the number of participating tubulin subunits. For example, calculating energies based on a separation at the level of atomic nuclei, a decoherence time of 500 ms is obtained for 10^9 participating tubulin, or about 10^3 neurons if it is assumed that 10% of the tubulin contained becomes involved (there are roughly 10^7 tubulin per neuron [43]). For a decoherence time of 25 ms (i.e., for coherent 40 Hz oscillations), 2×10^{10} tubulin, or about 20 000 neurons, would be involved. Orch. OR events with a decoherence time of 10^{-6} s would involve roughly 10^{14} tubulin, or about 10^8 neurons (approximately 0.1%–1% of the entire brain). A series of such fast orch. OR events could culminate in membrane depolarization or synaptic transmission.

TABLE I. Calculated values of some electrostatic properties of tubulin.

Tubulin property		Calculated value
Charge		$-10q_e$
Dipole moment		1714 D
Dipole	p_x	337 D
Moment	p_y	-1669 D
Components	p_z	198 D

terminal (C-terminus) domain, which probably constitutes the binding surface for motor proteins [44].

Recently, tubulin's electrostatic properties, including its potential energy surface, were calculated [45] with the aid of the molecular dynamics package TINKER. This computer program serves as a platform for molecular dynamics simulations and includes a facility to use protein-specific force fields. With the C-terminus tail excluded, the electrostatic properties of tubulin are summarized in Table I, following Brown [45].

Since 1 debye$=\frac{1}{3}\times10^{-29}$ C m, we find that the total dipole moment is approximately 5.7×10^{-27} C m, but only a fifth of it is oriented along the protofilament axis.[3]

It turns out that tubulin is quite highly negatively charged at physiological pH, but that much of the charge is concentrated on the C-terminus. This is the one portion of the tubulin dimer which was not imaged by Nogales *et al.* [44] due to its freedom to move following formation of the tubulin sheet. This tail of the molecule extends outward away from the microtubule and into the cytoplasm and has been described by Sackett [46]. At neutral *p*H, the negative charge on the carboxy terminus causes it to remain extended due to the electrostatic repulsion within the tail. Under more acidic conditions, the negative charge of the carboxy-terminal region is reduced by associated hydrogen ions. The effect is to allow the tail to acquire a more compact form by folding.

Any exposed charge in a cytoplasm will be screened by counterions forming a double layer. The screening distance provided by these counterions and water is the Debye length and, in the case of microtubules, its value is typically 0.6–1.0 nm under physiological conditions. Due to the exposure of negatively charged amino acids in the C terminus, a Debye layer is formed as shown in Fig. 3, screening thermal fluctuations due to the stronger Coulomb interactions over distances within the Debye length.

Ionic forces thus tend to cancel over even relatively short distances so that the forces mediating between tubulin and its environment should instead be characterized by dipolar interactions. This suggests that Tegmark's derivation of the decoherence time in Eq. (1) should be replaced with one that

[3]The x direction coincides with the protofilament axis. The α monomer is in the direction of increasing x values, relative to the β monomer. This is opposite to the usual identification of the β monomer as the "plus" end of the microtubule, but all this identifies is whether the microtubule is pointed towards or away from the cell body.

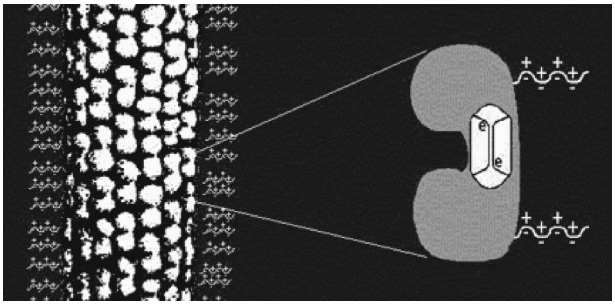

FIG. 3. Negative charges on the C-terminus tail of the tubulin dimer are screened under physiological conditions by counterions forming a Debye layer around the microtubule, as described by Sackett [46].

characterizes tubulin in terms of its electric dipole moment, thus avoiding the need to make a rather arbitrary cut in selecting which charges are to be constitutive of the overall charge of the kinked microtubule and which are to be neglected. Such a modification is accomplished by replacing the Coulomb potential, $V_{\text{Coulomb}}=q^2/4\pi\epsilon_0|\mathbf{r}_1-\mathbf{r}_0|$, describing the interaction of a quantum state of charge q at $\mathbf{r}_0$ and a similarly charged environmental ion at $\mathbf{r}_1$, in favor of a dipole potential, $V_{\text{dipole}}=q\mathbf{p}\cdot(\mathbf{r}_1-\mathbf{r}_0)/4\pi\epsilon_0|\mathbf{r}_1-\mathbf{r}_0|^3$, parametrized by $\mathbf{p}$, the electric dipole moment due to tubulin of the kinked microtubule. The interaction is well approximated, for the purposes of an order-of-magnitude estimate, by this dipole potential in the case that a, the distance between the environmental ion and the superposed state, is greater than the separation of charges in the determination of the electric dipole moment. This separation will not generally be larger than the length of a tubulin dimer, 8 nm, whereas $a=\frac{1}{2}D+n^{-1/3}\approx14$ nm for the same ionic density used by Tegmark, $n=\eta n_{\text{H}_2\text{O}}$ with $\eta\approx2\times10^{-4}$.

As in the Coulomb case of interacting charges, the force resulting from the dipole potential contributes only a phase factor in the evolution of the (reduced) density matrix, traced over the environmental degrees of freedom. These are thus tidal effects that determine the leading contribution to the rate of decoherence. In terms of the vector $\mathbf{a}\equiv\mathbf{r}_1^0-\mathbf{r}_0^0$, between the initial average positions of the environmental ion and the polarized quantum state, these tidal effects are given by the Hessian matrix of second derivatives of the interaction potential

$$\mathbf{M}=\frac{3qp}{4\pi\epsilon_0 a^4}[(5\hat{\mathbf{a}}\hat{\mathbf{a}}^T-\mathbf{I})(\hat{\mathbf{p}}\cdot\hat{\mathbf{a}})-(\hat{\mathbf{a}}\hat{\mathbf{p}}^T+\hat{\mathbf{p}}\hat{\mathbf{a}}^T)]. \tag{3}$$

Under the same assumptions that give rise to Eq. (1), the dipole case yields a decoherence time scale of

$$\tau\sim\frac{4\pi\epsilon_0 a^4\sqrt{mkT}}{3q_e ps}\Omega_{\text{dipole}}, \tag{4}$$

where

$$\Omega_{\text{dipole}}=(5\cos^2\theta\cos^2\varphi-4\cos\theta\cos\varphi\cos\psi+\cos^2\theta+\cos^2\varphi+\cos^2\psi)^{-1/2}$$

is a geometric factor fixed in terms of the angles between **p**, **a**, and **s**,

$$\cos\theta = \hat{\mathbf{a}}\cdot\hat{\mathbf{s}},$$

$$\cos\varphi = \hat{\mathbf{p}}\cdot\hat{\mathbf{a}},$$

$$\cos\psi = \hat{\mathbf{s}}\cdot\hat{\mathbf{p}}.$$

In our calculations, Ω_{dipole} is taken to be of order one.[4]

The calculation of the decoherence time scale in Eq. (4) can be made more realistic by taking into account the dielectric permittivity of tubulin in cytosol, neglected in the original calculation. Since the intracellular medium is primarily water, its dielectric constant can be quite high. The precise value of the permittivity of water is both temperature and frequency dependent but can be as high as $\epsilon \approx 80$ [47,48]. Conservatively estimating the dielectric constant of the surrounding medium by $\epsilon \approx 10$, and using the values given in Table I for the component of tubulin's electric dipole moment along the microtubule axis, together with the correction to the separation s discussed in Sec. II A, yields a decoherence time, $\tau \approx 10^{-5}$–10^{-4} s, that is already eight or nine orders of magnitude longer than that suggested by Tegmark, and sufficient for orch. OR events in the range of 10^{-6} s.

We also wish to point out that Mavromatos and Nanopoulos [38] estimated decoherence times for dipolar excitations in microtubules. Depending on the set of assumptions adopted, the value of τ obtained ranged from as low as 10^{-10} s using a conformal field theory method to as high as 10^{-4} s using a coherent dipole quantum state. For a kink state similar to that discussed by Tegmark, that value is of the order of 10^{-7}–10^{-6} s. Table II summarizes the relevant decoherence time scales.

TABLE II. Relevant decoherence time scales.

Proposed quantum superpositions	Calculated decoherence times
Superposition of neural firing (Tegmark)	10^{-20} s
Soliton superposition (Tegmark)	10^{-13} s
Orch. OR superpositions (corrected)	$10^{-5}-10^{-4}$ s
Coherent dipole state [38]	10^{-4} s
	of magnitude?

C. Dynamical time scales, shielding and error correction

Given the sizeable discrepancy between these estimates and those of Tegmark, it seems reasonable to reevaluate whether the assumptions and conclusions of his calculations are valid. In particular, the derivation requires that the decoherence time scale should fall far short of any relevant dynamical time scale for either the quantum object or the ionic environment, if the noninteracting contribution to the Hamiltonian is to be neglected relative to the interaction contribution. With the substantially modified decoherence times calculated above, this assumption is no longer justified, even by Tegmark's own estimates that place the dynamical time scale for a kinklike excitation traversing a microtubule at $\tau_{\text{dyn}} \approx 5 \times 10^{-7}$ s. The results of the derivation thus fail to be consistent with its assumptions, and Tegmark's formulation of the decoherence time must be rejected as inappropriate to the superposition under consideration. Without this crucial assumption validated, Tegmark's calculation fails to achieve self-consistency in the approximation regime considered, and must be rejected as inappropriate to the superpositions of interest in the orch. OR theory.

Two possible avenues might be envisioned in the framework of the orch. OR theory by which to overcome the influence of decoherence due to scattering and tidal effects, such that decoherence by quantum gravitational effects might play a role. The most obvious solution is to require that the shortest decoherence times be those due to quantum gravity. An equally viable approach, however, is to require that decoherence due to other mechanisms be effectively countered by dynamical processes operating on time scales more rapid than that of the relevant form of decoherence. This is the means by which quantum systems, such as lasers, maintain quantum coherence against thermal disruption at room temperature. The lasing phenomenon is about a supply of energy that is transformed from incoherent to coherent form, with an attendant reduction in entropy and increase in order. The introduction of nonequilibrium conditions impacts decisively on the conclusions that one might derive from calculations of the decoherence rate, which assume that equilibrium conditions hold sway. The significance of nonequilibrium situations in addressing phenomena in living media—decidedly not in equilibrium—cannot be overstated. Whereas the dynamical time scale for lasers is determined by the rate at which the system is pumped by an incoherent source of energy, appropriate dynamical time scales in the microtubule case might be determined by the characteristic rates at which incoherent metabolic energy is provided to processes that might counteract decoherence by scattering, such as actin gelation in sol-gel cycles and the ordering of water, both discussed below. Relevant rates could include that of GTP hydrolysis (known to control the stability of microtubules [49,50]), dephosphorylation of microtubule-associated proteins, and ATP hydrolysis (required for actin polymerization).

The transition between the alternating phases of solution and gelation in cytoplasm depends on the polymerization of actin (see Fig. 4), and the particular character of the actin gel in turn depends on actin cross linking. Of the various cross-linker related types of gels, some are viscoelastic, but others (e.g., those induced by the actin cross-linker avidin) can be

[4]Though Ω_{dipole} increases without bound as the three vectors, $\hat{\mathbf{a}}$, $\hat{\mathbf{p}}$, and $\hat{\mathbf{s}}$, approach mutual orthogonality, randomly oriented vectors rarely come close enough to satisfying this condition to make an order of magnitude difference in the decoherence time.

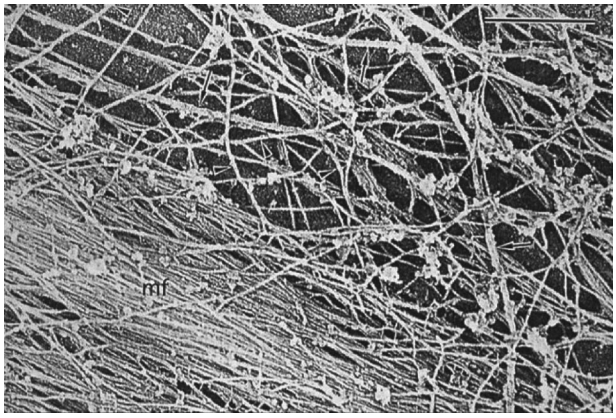

FIG. 4. Immunoelectron micrograph of cytoplasm showing microtubules (arrows), intermediate filaments (arrowheads), and actin microfilaments (mf). A dense actin gel (lower left) completely obscures the microtubules below. Scale bar at upper right represents 500 nm. With permission from Svitkina *et al.* [80].

deformed by an applied force without response [51]. Cycles of actin gelation can be rapid [52], and in neurons, have been shown to correlate with the release of neurotransmitter vesicles from presynaptic axon terminals [53,54]. In dendritic spines, whose synaptic efficacy mediates learning, rapid actin gelation and motility mediate synaptic function, and are sensitive to anesthetics [55–57].

In the orch. OR model, actin gelation encases microtubules during their quantum computation phase. Afterwards, the gel liquifies to an aqueous form suitable for communication between microtubule states and the external environment. Such alternating phases can explain how input from, and output to, the environment can occur without disturbing quantum isolation.

The water within cells is itself not truly liquid, but has been shown to be, to a large extent, ordered [58]. Most of the ordered water in the cell in fact surrounds the cytoskeleton [59]. Neutron diffraction studies indicate several layers of ordered water on such surfaces, with several additional layers of partially ordered water. Tegmark himself allows that the dynamical process of ordering water in the vicinity of the microtubule[5] could protect the quantum system from short-range sources of decoherence, such as the scattering of nearby molecules.

In fact, there is a long history to the hypothesis that macroscopic quantum coherence might be supported biologically by maintaining a supply of energy at a rate exceeding a threshold value [60–62]. The collective effects responsible for the ordering of water arise in the context of a supply of metabolic energy [58]. Empirical evidence indicates that, in the presence of an activation energy approximating the amount required for the formation of a soliton on the microtubule ($\approx$0.3 eV), the surrounding water can be easily brought to an electret state [63,64]. Spontaneous breaking of the dipole rotational symmetry in the interaction of the electric dipole moment of water molecules with the quantized electromagnetic field would then give rise to the dipolar wave quanta that are postulated to mediate collective effects [65–67].

In the gel phase, the water-ordering surfaces of a microtubule are within a few nanometers of actin surfaces that also order water. Thus bundles of microtubules encased in actin gel may be effectively isolated with the decoherence-free zone *a* extending over the radius of the bundle, of the order of hundreds of nanometers. If the *a* dependence of the decoherence time is accurately reflected in the previously corrected version (4) of Tegmark's equation, an order of magnitude increase in the decoherence-free zone results in an increase of three orders of magnitude in the decoherence time for the microtubule bundle.

Technological quantum computing is, in general, feasible because of the use of quantum error correction codes. It has been suggested that error correction may be facilitated by topologies—for instance, toroidal surfaces [68,69]—in which global, topological degrees of freedom are protected from local errors and decoherence. Topological quantum computation and error correction have been suggested in microtubules.[6]

D. Temperature dependence

An examination of the temperature dependence in the formulation of decoherence time casts further doubt on the validity of the reasoning that led Tegmark to claim an ultrarapid decoherence rate due to long-range forces. If the adoption of Eq. (1), even in the modified form, Eq. (4), were justified, it would require that the decoherence time be a monotonically *increasing* function of temperature; decoherence times would tend to grow as the square root of temperature. The apparent implication is that one should expect to find longer-lived quantum coherent states at higher temperatures, contrary to the intuition from thermodynamics, statistical mechanics, and kinetic theory, that increased thermal agitation should have a disruptive effect on the formation and preservation of quantum coherence (at least in thermal equilibrium, the only paradigm considered in [41]).

It might be objected that this intuition proceeds from a consideration of the increased impact of ionic and radiative

[5]While the point is conceded with respect to the water *inside* the microtubule, Tegmark finds it more contentious as regards the water *outside* the microtubule, which ''fills the entire cell volume.'' Geometric considerations aside, the mechanism of ordering is independent of whether the water is inside or outside the microtubule, and is only contended for the water closely approaching the microtubule.

[6]The microtubule lattice features a series of helical winding patterns that repeat on longitudinal protofilaments at 3,5,8,13,21 and higher numbers of subunit dimers (tubulins). These particular winding patterns (whose repeat intervals match the Fibonacci series) define attachment sites of the microtubule-associated proteins (MAPs), and are found in simulations of self-localized phonon excitations in microtubules [70]. They suggest topological global states in microtubules which may be resistant to local decoherence [71]. Penrose [72] has suggested that the Fibonacci patterns on microtubules may be optimal for error correction.

(see subsequent Sec. II E) scatterers at higher temperatures. Since we are investigating tidal influences of long-range forces, influences that are not amenable to formulation in terms of scattering states, one might choose to disregard such intuitions. Noting that it is only the shortest decoherence time, amongst those calculated for competing decohering processes, that will be observable, it might be argued that a counterintuitive temperature dependence in the decoherence rate due to a particular process would remain invisible if this rate were not the fastest. For instance, if the decoherence rate, R_s due to a species of scatterers beat the decoherence rate R_d, due to the tidal influence of distant ions, we would have no physical indication of the temperature dependence in R_d. While this allows us to preserve our physical intuitions, it defeats the purpose of calculating R_d. In [41], R_d is calculated because it is expected to be the dominant rate given that R_s is suppressed by the ordering of water near microtubules.

Nevertheless, it might be contended that R_d dominates decoherence only within a range of temperatures that does not include very low temperatures—where our experience with quantum coherent states argues against the counterintuitive temperature dependence in Eq. (1)—and also does not include very high temperatures, where thermal considerations must eventually reassert themselves over other effects. This could only be maintained, however, if the temperature dependence in R_d were not monotonic and increasing without bound in the low temperature limit (as is Tegmark's). In that case, R_d would eventually overtake R_s as temperature decreases, with the result that we would not observe the longest-lived quantum superpositions at the lowest temperature. Further, it does not seem possible, in order to escape this conclusion, to claim that the temperature dependence in R_s is also counterintuitive since this is precisely the case in which we must expect the strictures of thermodynamics and statistical mechanics to be binding. It should be noted in this context that even the formulas derived in [41] to account for the effect of scattering determine decoherence times that increase with increasing temperature, rather than decrease.

Tegmark's Eq. (1) suggests that low temperatures, at which decohering environmental interactions presumably have the least impact, are deemed most inhospitable to quantum coherence, contrary to experience. Though the equation is formulated to be valid at room temperature, the stated assumptions appear to remain valid in the low temperature limit. Both object and environment should be well localized in this limit and, unless it is imagined that the dynamical time scale goes to zero in the low temperature limit even more rapidly than the decoherence scale—entailing a dynamical rate that increases without bound as absolute zero is approached—the requirement that the decoherence scale must lie well below the dynamical scale is also met. Accounting for the temperature dependence implicit in a, which must decrease to a minimum in the absence of thermal agitation, only exacerbates the counterintuitive trend.

While the equations derived in [41] in the case of ion-ion and ion-water scattering do not exhibit the expected temperature dependence over the range of temperatures in which they are deemed valid, it may be possible to recover the appropriate dependence in the low temperature limit. The approximation regime valid at room temperature will no longer be appropriate in the low temperature limit since the de Broglie wavelength λ of the scatterer is no longer expected to be much smaller than the superposition separation s of the quantum state. Making the alternate approximation, $s \ll \lambda$, which should be valid at sufficiently low temperatures, the ion-water scattering case recovers the intuitive temperature dependence, but the ion-ion scattering case does not, suggesting that the problems in the derivation lie deeper. Even in the ion-water case, adjusting the approximation regime relieves the counterintuitive temperature dependence only at temperatures near absolute zero. Moreover, in the case of interest here—that of decoherence due to tidal influences of long-range forces—there is no analogous approximation to adjust at low temperatures.

Regardless of any deviations from the predicted trend that might mitigate the failure of the low temperature limit in the neighborhood of absolute zero, the functional dependence of the decoherence time, across the range of temperatures in which the calculation is deemed valid (and in particular at room temperature), runs contrary to the expectation that the onset of decoherence should, in general, be more rapid at higher temperatures.

E. Other mechanisms of decoherence

Since any process that irreversibly conveys a flow of information from the system to the environment acts as a source of decoherence, our remarks concerning the threat of decoherence through the tidal effects of long-range forces, while addressing an important source of decoherence, clearly do not exhaust the potential for disruptive environmental influence. In particular, we would like to have some quantitative estimate of the decoherence time associated with ubiquitous radiative scatterers.

A decoherence formalism for apparent wave function collapse due to scattering has been developed in [73], and is summarily reviewed below. The treatment adopts the assumption that the interaction between the system and scatterer can be treated as approximately instantaneous relative to the dynamical time scales of the Hamiltonian governing the evolution of the system. Note that in this approximation, it is these interaction times (this might be given by the transit time of the scatterer through the system), not decoherence times, that are presumed short in comparison to dynamical times, and hence this is not the same approximation whose validity was questioned in Sec. II C.

The change in the density matrix ρ for the system and scatterer together is given in terms of a transition matrix T by $\rho \rightarrow \rho' = T\rho T^{\dagger}$. If T conserves energy and momentum, then the transition matrix element has the form

$$\langle \mathbf{p}'\mathbf{k}' | T | \mathbf{p}\mathbf{k} \rangle = \delta(\mathbf{p}' + \mathbf{k}' - \mathbf{p} - \mathbf{k}) a_{\mathbf{pk}}(\mathbf{p}' - \mathbf{p}), \qquad (5)$$

where $|\mathbf{pk}\rangle$ denotes the state in which the system has momentum $\mathbf{p}$ and the scatterer has momentum $\mathbf{k}$, and $a_{\mathbf{pk}}(\mathbf{p}' - \mathbf{p})$ is the probability amplitude for a momentum transfer to the system of $\mathbf{p}' - \mathbf{p}$. If the velocity of the incident scatterer is much greater than the spread of velocities in the density

matrix (which will generally be the case for the types of scatterers to be considered subsequently), the probability amplitude can be treated as independent of **p**. With the further assumption that the incident particle is in a momentum eigenstate or an incoherent mixture of momentum eigenstates, it is shown in [73] that the effect of such a scattering event on the density matrix is

$$\rho(\mathbf{x},\mathbf{x}') \rightarrow \rho'(\mathbf{x},\mathbf{x}') = \rho(\mathbf{x},\mathbf{x}')\hat{P}(\mathbf{x}'-\mathbf{x}), \tag{6}$$

where $\hat{P}(\mathbf{x}'-\mathbf{x})$ is the Fourier transform of

$$P(\mathbf{p}'-\mathbf{p}) = \int |a_{\mathbf{k}}(\mathbf{p}'-\mathbf{p})|^2 \mu(\mathbf{k}) d^3k, \tag{7}$$

representing an incoherent superposition of plane waves with momentum probability distribution $\mu(\mathbf{k})$. A generic anisotropic spectrum $\mu(\mathbf{k})$ will result in radiation pressure, itself a potential source of decoherence [74]. Forces due to radiation pressure, however, are in general significantly weaker than those due to scattering and are unlikely to yield a faster rate of decoherence. Consideration is thus limited to an isotropic spectrum,

$$\mu(k) = \lambda_0 \nu(\lambda_0 k)/4\pi k^2, \tag{8}$$

where $k = |\mathbf{k}|$, λ_0 is a characteristic wavelength and ν is a probability distribution over the real line. In particular, we will be interested in the Planck distribution

$$\nu(x) = \frac{1}{2\zeta(3)} \frac{x^2}{e^x - 1} \tag{9}$$

for radiative scatterers in ambient visible light, in the flux of thermal radiation from our surroundings, and in the cosmic microwave background radiation, spectra corresponding to blackbody temperatures of 5800 K, 300 K, and 2.7 K, respectively.

With a flux Φ of scatterers and a total cross section σ the incidence of scattering events is governed by a Poisson distribution with intensity, $\Lambda = \sigma\Phi$. If it were scattering processes alone that evolved the density matrix, it would thus be subject to

$$\dot{\rho}(\mathbf{x},\mathbf{x}',t) = -\Lambda(1-\hat{P}(\mathbf{s}))\rho(\mathbf{x},\mathbf{x}',t), \tag{10}$$

where we have defined $\mathbf{s} = \mathbf{x}' - \mathbf{x}$. If the time scale given by Λ^{-1} is short compared to all the dynamical time scales in the system Hamiltonian, this is approximately the case that prevails. The solution to Eq. (10),

$$\rho(\mathbf{x},\mathbf{x}',t) = \rho(\mathbf{x},\mathbf{x}',t_0) e^{-\Lambda t(1-\hat{P}(\mathbf{s}))}, \tag{11}$$

will then adequately capture the behavior of the density matrix for the short times over which the usual Schrödinger evolution can be neglected.

In the isotropic case, the mean of the distribution, $\hat{P}(\mathbf{s})$, vanishes and the covariance matrix is proportional to the identity matrix, $S_{ij} = v\,\delta_{ij}$ with the constant of proportionality given by the variance v. This allows us to make the following Gaussian approximation in the solution above:

$$\rho(\mathbf{x},\mathbf{x}',t) \approx \rho(\mathbf{x},\mathbf{x}',t_0)\exp[-\Lambda t(1-e^{-s^2/2\lambda_{\text{eff}}^2})], \tag{12}$$

where $s = |\mathbf{s}|$ is the superposition separation of Sec. II A, and $\lambda_{\text{eff}} = 1/\sqrt{v}$ is given by

$$\lambda_{\text{eff}} = \frac{\lambda_0}{\sqrt{-g''(0)\langle x^2\rangle}}. \tag{13}$$

Here, $\langle x^2\rangle = 4!\zeta(5)/2!\zeta(3)$, denotes the expectation value of x^2 over the Planck distribution $\nu(x)$, and the function

$$g(x) = \frac{\sin x}{x} \int_0^{2\pi} \int_{-1}^{1} e^{\imath x u} f(\arccos u, \varphi) du d\varphi \tag{14}$$

results from the Fourier integral in $\hat{P}(\mathbf{s})$ over the momentum probability distribution in Eq. (8), such that

$$\hat{P}(\mathbf{s}) = \int_0^\infty g\left(\frac{ws}{\lambda_0}\right) \nu(w) dw. \tag{15}$$

The differential cross section $f(\theta,\varphi)$ in Eq. (14) has been normalized so as to integrate to 1. In the case of *s*-wave scattering, appropriate for treating opaque systems much larger than the wavelength of the scattering photons, $f(\theta,\varphi) = 1/4\pi$, so $g(x) = \sin^2 x/x^2$ and $g''(0) = -2/3$. According to Eq. (13), one then calculates $\lambda_{\text{eff}} = 0.381\lambda_0$. In the case of photons scattering from dielectric spheres much smaller than the wavelength of the photons, the appropriate normalized differential cross section [75] is $f(\theta,\varphi) = 3(1 + \cos^2\theta)/16\pi$, which determines

$$g(x) = \frac{3\sin x}{2x^3}\left(\cos x + (x^2-1)\frac{\sin x}{x}\right), \tag{16}$$

and $g''(0) = -11/15$. The effective wavelength in this case is then $\lambda_{\text{eff}} = 0.363\lambda_0$.

In the near-diagonal approximation appropriate when $s \ll \lambda_{\text{eff}}$, the solution in Eq. (12) reduces to

$$\rho(\mathbf{x},\mathbf{x}',t) \approx \rho(\mathbf{x},\mathbf{x}',t_0)\exp(-\Lambda s^2 t/2\lambda_{\text{eff}}^2), \tag{17}$$

which identifies the decoherence time as

$$\tau \sim \frac{\lambda_{\text{eff}}^2}{\Lambda s^2}. \tag{18}$$

Table III summarizes estimates, adapted from [73], for Λ, Φ, and λ_{eff} for each of the scattering sources under consideration, and gives values of τ calculated on the basis of Eq. (18). For Λ and τ the results are expressed over a range extending from the case of a single electron in superposition to that of a mote 10 μm in size. The cross section σ for interaction with an electron is estimated at roughly 5×10^{-29} m^2, and for interaction with a 10 μm mote at 5×10^{-10} m^2. Even in the case of a superposed system as

TABLE III. Characteristic values, adapted from [73], for several scattering processes. Decoherence times are quoted in the near-diagonal approximation $\tau=\lambda_{\mathrm{eff}}^2/\Lambda s^2$ appropriate to the superposition separations, s, given in Sec. II A.

		Ambient visible light	300 K photons	Cosmic microwaves
Λ (s^{-1})	Electron	5×10^{-8}	5×10^{-6}	5×10^{-12}
	10 μm mote	5×10^{11}	5×10^{13}	5×10^{7}
Φ (m^{-2} s^{-1})		10^{21}	10^{23}	10^{17}
λ_{eff} (m)		9×10^{-7}	2×10^{-5}	2×10^{-3}
τ (s)	Electron	10^{25}	10^{26}	10^{36}
	10 μm mote	10^{6}	10^{7}	10^{17}

large as 10 μm, decoherence times due to radiative scatterers are substantially longer than those postulated to result from the effects of quantum gravity in the orch. OR theory, a result attributable to the fact that the superposition separation is so small. The decohering effect of radiative scatterers thus does not appear to pose a significant threat to the proposed mechanism.

III. OUTLOOK

Among the many features of brain function not currently understood, subjectivity remains the most problematic, motivating both classical and quantum explanations. Quantum approaches, in particular the orch. OR model in microtubules, are potentially able to account for features like the unified nature of conscious experience and subjectivity [76–78], but are based on speculative quantum level activities and appear on the surface to suffer from a decoherence problem.

The mechanisms of decoherence discussed here, however, fail to rule out biologically instantiated quantum coherence of the sort envisioned in the orch. OR hypothesis, particularly when proposed biological mechanisms of coherent pumping, screening, and quantum error correction are considered. When appropriately revised, both theoretically and numerically, decoherence times due to the tidal influence of Coulomb forces appear to be in line with the relevant dynamical times, in the range 10^{-5}–10^{-4} s, in accord with biological phenomena. These revisions place the microtubule decoherence time in a range invalidating Tegmark's assumption that the decoherence time scale is much shorter than relevant physiological dynamical time scales, and suggest that the approximation scheme used is inappropriate to the superposition under consideration. Further, the temperature dependence of Tegmark's formulation fails to confirm, in the case of both tidal influences of Coulomb forces and decoherence due to scattering, the intuition that increased thermal disruption should have a deleterious effect on the formation and maintenance of quantum coherent states. These intuitions are expected to be particularly robust in thermal equilibrium, which is the context that Tegmark considers. Consideration of other mechanisms of decoherence, such as that due to radiative scattering, indicate that these play no role in the determination of the decoherence rate. Thus the issue of organized quantum processes in the brain remains open, and subject to experimental verification, an indication that there is cause for optimism that some of the enigmatic features of the cognitive processes occurring in consciousness might yet be understood in a quantum theoretical framework.

ACKNOWLEDGMENTS

S.H. and S.R.H. would like to thank Gerard Milburn for helpful discussions. J.A.T. acknowledges support from NSERC, PIMS, and MITACS. S.H. and J.A.T. wish to express their gratitude for research support from the Center for Consciousness Studies at the University of Arizona. S.R.H. appreciates support from the Fetzer Institute, the YeTaDel Foundation, and Biophan. All authors are indebted to Roger Penrose for the formulation of the ideas under discussion and to Dave Cantrell for illustrations.

[1] J.J. Hopfield, Proc. Natl. Acad. Sci. U.S.A. **81**, 2554 (1982).
[2] J.J. Hopfield, Phys. Today **47** (2), 40 (1994).
[3] W.A. Little, Math. Biosci. **19**, 101 (1974).
[4] G. Parisi, J. Phys. A **19**, L617 (1986).
[5] T. Khanna, *Foundations of Neural Networks* (Addison-Wesley, New York, 1990).
[6] A. Lewis and L. V. del Priore, Phys. Today **41** (1), 38 (1988).
[7] D.A. Baylor, T.D. Lamb, and K.W. Yau, J. Physiol. (London) **288**, 613 (1979).
[8] W. Denk and W.W. Webb, Phys. Rev. Lett. **63**, 207 (1989).
[9] F. Beck and J.C. Eccles, Proc. Natl. Acad. Sci. U.S.A. **89**, 11 357 (1992).
[10] G. Liu and J.L. Feldman, J. Neurophysiol. **68**, 1468 (1992).
[11] A. Larkman, K. Stratford, and J. Jack, Nature (London) **353**, 396 (1991).
[12] A. S. Davydov, *Biology and Quantum Mechanics* (Pergamon Press, Oxford, 1982).
[13] A. Roitberg, R.B. Gerber, R. Elber, and M.A. Ratner, Science **268**, 1319 (1995).
[14] J. Tejada *et al.*, Science **272**, 424 (1996).
[15] W.S. Warren *et al.*, Science **281**, 247 (1998).
[16] R.R. Rizi *et al.*, Magn. Reson. Med. **43**, 627 (2000).
[17] W. Richter *et al.*, Magn. Reson. Imaging **18**, 489 (2000).
[18] J.R. Searle, Behav. Brain Sci. **3**, 417 (1980).
[19] W. James, *The Principles of Psychology* (Holt, New York, 1890).
[20] R. Penrose, *Shadows of the Mind* (Oxford University Press, New York, 1994).
[21] R. Penrose, Int. Stud. Philos. Sci. **11**, 7 (1997).
[22] R. Penrose and S.R. Hameroff, J. Conscious. Stud. **2**, 98 (1995).
[23] S.R. Hameroff and R. Penrose, J. Conscious. Stud. **3**, 36 (1996).

[24] S.R. Hameroff, Philos. Trans. R. Soc. London Ser. A **356**, 1869 (1998).
[25] P. Dustin, *Microtubules* (Springer-Verlag, New York, 1984).
[26] S.R. Hameroff and R.C. Watt, J. Theor. Biol. **98**, 549 (1982).
[27] S. R. Hameroff, *Ultimate Computing* (North-Holland, Amsterdam, 1987).
[28] S. Rasmussen *et al.*, Physica D **42**, 428 (1990).
[29] M.V. Satarić, J.A. Tuszyński, and R.B. Zakula, Phys. Rev. E **48**, 589 (1993).
[30] J. Dayhoff, S. Hameroff, R. Lahoz-Beltra, and C. E. Swenberg, Eur. Biophys. J. **23**, 79 (1994).
[31] J.A. Tuszyński *et al.*, J. Theor. Biol. **174**, 371 (1995).
[32] J.A. Tuszyński, B. Trpišová, D. Sept, and M.V. Satarić, BioSystems **42**, 153 (1997).
[33] M. Conrad, Chaos, Solitons Fractals **4**, 423 (1994).
[34] D. Voet and J. G. Voet, *Biochemistry*, 2nd ed. (Wiley, New York, 1995).
[35] N.P. Franks and W.R. Lieb, Nature (London) **310**, 599 (1984).
[36] S.R. Hameroff, Toxicol. Lett. **100**, 31 (1998).
[37] N. Mavromatos and D.V. Nanopoulos, Int. J. Mod. Phys. B **11**, 851 (1997).
[38] N. Mavromatos and D.V. Nanopoulos, Adv. Struct. Biol. **5**, 283 (1998).
[39] N. J. Woolf, Conscious. Cogn. **6**, 574 (1997).
[40] P. Zizzi (private communication).
[41] M. Tegmark, Phys. Rev. E **61**, 4194 (2000).
[42] S. R. Hameroff and R. Penrose, in *Toward a Science of Consciousness—The First Tucson Discussions and Debates*, edited by S. R. Hameroff, A. W. Kaszniak, and A. C. Scott (MIT Press, Cambridge, MA, 1996), pp. 507–540.
[43] W. Yu and P.W. Baas, J. Neurosci. **14**, 2818 (1998).
[44] E. Nogales, S. Wolf, and K. Downing, Nature (London) **91**, 199 (1998).
[45] J. A. Brown, Ph.D. thesis, University of Alberta, Edmonton, 1999.
[46] D. Sackett, Subcellular Biochemistry **24**, 255 (1995).
[47] J. B. Hasted, *Aqueous Dielectrics* (Chapman and Hall, London, 1973).
[48] J.A. Tuszyński, D. Sept, and J.A. Brown, Can. J. Phys. **53**, 237 (1997).
[49] A.A. Hyman *et al.*, Mol. Biol. Cell **3**, 1155 (1992).
[50] A.A. Hyman, D. Chrétien, I. Arnal, and R.H. Wade, J. Cell Biol. **128**, 117 (1995).
[51] D. H. Wachsstock, W.H. Schwarz, and T.D. Pollard, Biophys. J. **66**, 801 (1994).
[52] J. Xu, D. Wirtz, and T.D. Pollard, J. Biol. Chem. **273**, 9570 (1998).
[53] S. Miyamoto, Biochim. Biophys. Acta **1244**, 85 (1995).
[54] S. Muallem, K. Kwiatkowska, X. Xu, and H.L. Yin, J. Cell Biol. **128**, 589 (1995).
[55] S. Kaech, M. Fischer, T. Doli, and A. Matus, J. Neurosci. **17**, 9565 (1997).
[56] M. Fischer, S. Kaech, D. Knutti, and A. Matus, Neuron **20**, 847 (1998).
[57] S. Kaech, H. Brinkhaus, and A. Matus, Proc. Natl. Acad. Sci. U.S.A. **96**, 10 433 (1999).
[58] J.S. Clegg, Am. J. Phys. **246**, R133 (1984).
[59] J. Clegg, Collect. Phenom. **3**, 289 (1981).
[60] H. Fröhlich, Int. J. Quantum Chem. **2**, 641 (1968).
[61] H. Fröhlich, Nature (London) **228**, 1093 (1970).
[62] H. Fröhlich, Proc. Natl. Acad. Sci. U.S.A. **72**, 4211 (1975).
[63] S. Celaschi and S. Mascarenhas, Biophys. J. **20**, 273 (1977).
[64] J.B. Hasted, H.M. Millany, and D. Rosen, J. Chem. Soc., Faraday Trans. 2 **77**, 2289 (1981).
[65] E. del Guidice, S. Doglia, M. Milani, and G. Vitiello, Nucl. Phys. B **251**, 375 (1985).
[66] E. del Guidice, S. Doglia, M. Milani, and G. Vitiello, Nucl. Phys. B **275**, 185 (1986).
[67] M. Jibu *et al.*, BioSystems **32**, 195 (1994).
[68] A.Y. Kitaev, e-print quant-ph/9707021.
[69] S.B. Bravyi and A.Y. Kitaev, e-print quant-ph/9811052.
[70] A. Samsonovich, A. Scott, and S. Hameroff, Nanobiology **1**, 457 (1992).
[71] M. J. Porter (private communication).
[72] R. Penrose (private communication).
[73] M. Tegmark, Found. Phys. Lett. **6**, 571 (1993).
[74] P.A.M. Neto and D.A.R. Dalvit, e-print quant-ph/0004057.
[75] J. D. Jackson, *Classical Electrodynamics* (Wiley, New York, 1975), p. 414.
[76] I.N. Marshall, New Ideas Psychol. **7**, 73 (1989).
[77] H. P. Stapp, *Mind, Matter, and Quantum Mechanics* (Springer-Verlag, Berlin, 1993).
[78] A. J. Cairns-Smith, *Evolving the Mind: On the Nature and the Origin of Consciousness* (Cambridge University Press, Cambridge, 1996).
[79] N. Hirokawa, in *The Neuronal Cytoskeleton*, edited by R. Burgoyne (Wiley, New York, 1991).
[80] T. M. Svitkina, A. B. Verkhovsky, and G. G. Borisy, in *Recent Advances in Microscopy of Cells, Tissues and Organs*, edited by M. Malpighi and P. M. Motta (Antonio Delfino Editore, Rome, 1997), pp. 93–100.